ELSEVIER

Superlattices and Microstructures 38 (2005) 201–208

Superlattices and Microstructures

www.elsevier.com/locate/superlattices

Broadening of terahertz spectrum due to Zener tunnelling in superlattices

Peng Han, Kui-juan Jin*, Yueliang Zhou, Qing-li Zhou, Hui-bin Lu, Dong-yi Guan, Zheng-hao Chen

Beijing National Laboratory for Condensed Matter Physics, Institute of Physics, Chinese Academy of Sciences, Beijing 100080, China

Received 11 April 2005; received in revised form 19 July 2005; accepted 21 July 2005
Available online 8 August 2005

Abstract

The resonant interminiband Zener tunnelling rates between two minibands in the process of terahertz (THz) radiation have been calculated for three structures of $GaAs/Al_{0.3}Ga_{0.7}As$ superlattices with high electric field in this work by using the Kane model. It is found that Zener tunnelling rate, which corresponds to the broadening of line-width of spectrum, not only increases with the applied electric field F but also is very dependent on the width of the minibands and that of the gap between minibands. Without any fitting parameter, the calculated results agree with the experimental data reported by Prof. Hirakawa and his co-workers. The results we obtained in this work demonstrate that the measured broadening in the spectra of terahertz emission in the high electric field region is indeed due to the resonant interminiband Zener tunnelling.

PACS: 73.21.Cd; 73.40.-c; 78.47.+p

Keywords: THz emission; Superlattice; Zener tunnelling

* Corresponding author. Tel.: +86 10 8264 8099; fax: +86 10 8264 8099.
E-mail address: kjjin@aphy.iphy.ac.cn (K.-j. Jin).

0749-6036/$ - see front matter © 2005 Elsevier Ltd. All rights reserved.
doi:10.1016/j.spmi.2005.07.002

1. Introduction

Terahertz (THz) radiation, having a frequency between microwave and laser, has a number of highly interesting applications in biological imaging, surface chemistry, and high-field condensed matter studies [1]. There are many methods such as synchrotron radiation [2], transition radiation [3] and frequency up-conversion of electromagnetic radiation [4] to generate THz radiation. In 1993, THz emission was first observed from Bloch Oscillations (BOs) in a superlattices (SLs) using time-resolved THz emission spectroscopy [5]. Till now, considerable effort in experimental [6–11] and theoretical aspects [12,13] has been made to investigate this topic. Recently, it has been proved that the THz radiation can be generated by BOs in SLs from the theoretical aspect [12]. In an ideal periodic system, when only one band is considered and electron scattering is neglected, BOs would last forever. However, in a real system, the damping of BOs will affect the carrier transport in SLs and the THz radiation [11]. Therefore, it is very important to clarify the effect of the damping of BOs on the THz emission spectra.

With the increasing of electric field, coupling to the higher minibands (Zener tunnelling) will damp BOs when the higher minibands are considered. It is well known that the quantity $\hbar\gamma$, where γ is the Zener tunnelling rate, can be considered as the imaginary part of the eigenvalues. This part leads to an exponential decay of the probability of the wave function and to the broadening in the emission spectra, corresponding to the half width at half maximum (HWHM) of the THz emission spectrum. In addition, the phenomenon that the spectral shape drastically changes and becomes very broad at a certain applied field has been assumed to be due to the resonant interminiband Zener tunnelling in Ref. [8].

In his famous work [14], Zener first proposed the concept of Zener tunnelling and calculated the tunnelling rate based on a semiclassical approach. Then considerable effort was made to study this tunnelling in experimental [15–17] and theoretical aspects [18, 19]. Recently, Glutsh [20] has derived a formula from the Kane model to calculate Zener tunnelling rate. This method has been proved to be good enough when electric field is below 60 kV/cm for the optical absorption spectrum experiment with the system he treated [20].

In this work, we calculated the resonant interminiband Zener tunnelling rate in three structures of $GaAs/Al_{0.3}Ga_{0.7}As$ SLs under an applied electric field F using the method mentioned in Ref. [20]. Comparison between our theoretical results and the experimental data from Ref. [8] has been made, and a good agreement between our calculated Zener tunnelling rates and measured HWHM of the THz spectrum has been obtained. This result gives evidence that the broadening of spectra in the high field region (from about 14 to 21 kV/cm) is indeed due to the coupling of two minibands.

2. Theoretical model

The studied system is the undoped $GaAs/Al_{0.3}Ga_{0.7}As$ SLs. In our work, the x axis is regarded as the growth direction of the SLs, $d = a + b$ is the periodicity of the SLs, where a is the well width and b is the barrier width. In addition, $V(x) = V(x + ld)$ is the one dimensional lattice-periodic potential. Setting the zero reference energy at the bottom of the GaAs conduction band edge, the barrier height is 250 meV. To model these SLs of

finite length, we regard ld as the positions of the centers of the wells with $l = 1, 2, \ldots, m$, where m is the total number of the SLs' periods. The Hamiltonian H of an electron with charge $-e$ in the SLs under an applied field F in the x axis of the SLs is expressed as

$$H = -\frac{\hbar^2}{2\mu}\frac{\mathrm{d}^2}{\mathrm{d}x^2} + V(x) + eFx \tag{1}$$

where, $\hbar$ is the reduced Planck constant and μ is the effective mass of the electron. For $F = 0$, the eigenfunctions of the Hamiltonian Eq. (1) can be written as Bloch functions,

$$\phi_{nk}(x) = \frac{1}{\sqrt{2\pi}}\mathrm{e}^{ikx}u_{nk}(x) \tag{2}$$

where, n is either 1 or 2 in this two-band model and k is the Bloch wave number. $u_{nk}(x)$ is the periodic part of the Bloch function, which can be written as $u_{nk}(x) = u_{nk}(x + ld)$. Then, we will use the basis of Bloch functions $\{\phi_{nk}(x)\}$ to solve our problem when the applied electric field is not equal to zero. For $F \neq 0$, the eigenfunctions of the Hamiltonian in Eq. (1) can be written as $\psi(x) = \sum_n \sum_{k\in BZ} a_n(k)\phi_{nk}(x)$.

The eigenvalues for the $a_n(k)$ can be solved by the following equation,

$$\left[E_n(k) + ieF\frac{\mathrm{d}}{\mathrm{d}k}\right]a_n(k) + eF\sum_{n'} X_{nn'}(k)a_{n'}(k) = \epsilon a_n(k) \tag{3}$$

where, $E_n(k)$ is the band energy of an electron in the periodic lattice without applied bias voltage F, and ϵ is the eigenvalue of the Hamiltonian in Eq. (1) with the electric field F. The interminiband coupling parameter $X_{nn'}(k)$ is defined as

$$X_{nn'}(k) = \frac{i}{d}\int_{-d/2}^{+d/2}\mathrm{d}x\,u^*_{nk}(x)\frac{\mathrm{d}u_{n'k}(x)}{\mathrm{d}k}.$$

Then the eigenvalue and eigenfunctions of Eq. (3) can be obtained with the Kane model [19,20].

The Zener tunnelling rate has been derived by Glutsch [20]:

$$\gamma = \frac{p(t)}{t} = \frac{eFd}{2\pi\hbar}\int_{-\pi/d}^{+\pi/d}\mathrm{d}k_1\int_{-\pi/d}^{+\pi/d}\mathrm{d}k_2\, f^*(k_1)g(k_1 - k_2, B)\, f(k_2) \tag{4}$$

where,

$$f(k) = X_{12}(k)\exp\left\{\frac{1}{ieF}\int_0^k \mathrm{d}k'[E_1(k') + eFX_{11}(k') - E_2(k') - eFX_{22}(k')]\right\}$$

and

$$g(k, B) = \sum_l \frac{\sin^2[(B - ld)\frac{\pi}{d}]}{[(B - ld)\frac{\pi}{d}]^2}\mathrm{e}^{i(B-ld)k}, \qquad B = \frac{\epsilon_{20} - \epsilon_{10}}{eF}.$$

So the HWHM $\hbar\gamma$, which has the dimension of energy, is obtained.

Table 1
The SL parameters and band structures for three structures

Parameters	Structure 1	Structure 2	Structure 3
SLs periods	47	55	73
Well width a (nm)	9.3	8.2	6.4
Barrier width b (nm)	1.3	0.8	0.56
First miniband (meV)	21–49	19–69	18–114
Second miniband (meV)	100–199	107–270	150–445
Band gap (meV)	51	38	36

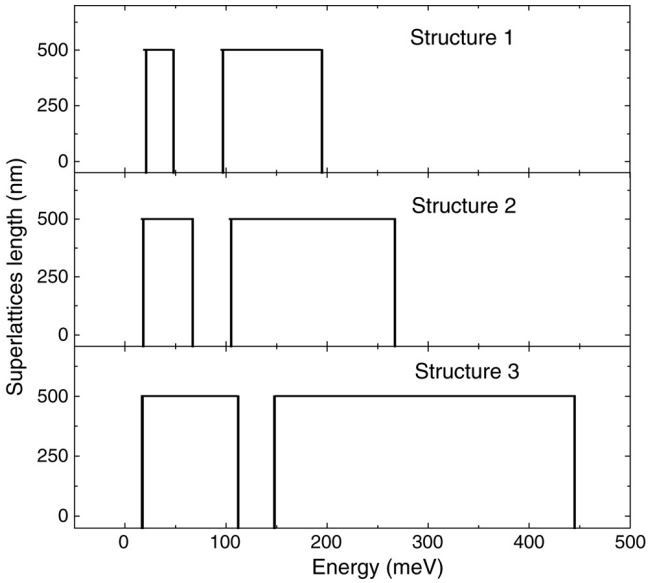

Fig. 1. Sketch of energy band for structure 1, 2, and 3.

3. Result and discussion

In order to study Zener tunnelling rate between two minibands with various energy band structures, we calculate three different SL structures. The SL parameters and the band structures of these three structures are summarized in Table 1. The eigenvalue problem of the Hamiltonian in Eq. (1) for $F = 0$ is solved with the Kronig–Penney model with a step size of $d/200$ and the Brillouin zone is sampled by 2000 points. The energy band structures corresponding to structure 1, 2, and 3 are shown in Fig. 1. These three band structures we calculated are denoted as that structure 1 has the most narrow band miniband while the structure 3 has the widest one and the structure 1 has wider band gap than the other two.

The calculated curves of HWHM versus F are plotted in Fig. 2 for all those three structures. As shown in this figure, the shape of these curves agrees well with that of

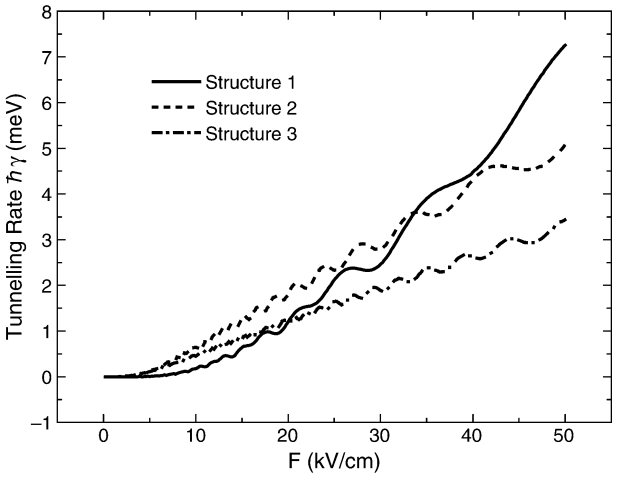

Fig. 2. The calculated Zener tunnelling rate $\hbar\gamma$ versus electric field F.

the calculated Zener tunnelling rate curves plotted in Ref. [20]. The results show that Zener tunnelling rates not only increase with the electric field, but also exhibit oscillations due to the result of the interaction between Wannier–Stark ladders (WSL) of the two minibands [20]. The function $g(k, B)$ in Eq. (4) is the source of these oscillations with period $eFd/(\epsilon_{20} - \epsilon_{10})$. From Fig. 2, we can also find that the periods of oscillations increase with the electric field. When the electric field F is not very large, $eFX_{nn'}$ is much less than $E_n(k)$. Thus, ϵ_{10} and ϵ_{20} can be taken as the average energies of the first and the second minibands, respectively. Therefore the structure with wider bandwidth has smaller period of the oscillation in the case that the miniband gaps are comparable for these different structures as shown in Fig. 2. Here, we define $\epsilon_{20} - \epsilon_{10}$ as the average energy difference $\Delta\epsilon$. The values of $\Delta\epsilon$ for structure 1, 2, and 3 are about 113 meV, 149 meV and 242 meV, respectively. The periodicity d of SLs are 10.6 nm, 9.0 nm and 6.95 nm, respectively. Therefore, the oscillation period ratio of these three structures is about 3:2:1, which can be seen in Fig. 2. The widths of the minigap, which can be defined as the gap between the top of the first miniband and the bottom of the second miniband, are about 50 meV, 38 meV and 36 meV for structure 1, 2, and 3, respectively. So the width of minigap of structure 1 is larger than those of the others. Therefore, the Zener tunnelling rate of the structure 1 in the low field region is smaller than those of other structures. As the second miniband of structure 3 is largely above the barrier, the wave function of the second miniband in structure 3 is more delocalized than those of the others. Furthermore, the average values of the miniband coupling parameter X_{12} for structure 1, 2, and 3 are 8.776×10^{-4} cm, 6.323×10^{-4} cm, and 4.563×10^{-4} cm, respectively. Thus, the coupling between the two minibands of structure 3 is the least among these structures. So the Zener tunnelling rate of structure 3 is less than those of the others in the high field region. In addition, the interminiband tunnelling probability of structure 3 has also been proved very small with the Wentzel–Kramers–Brillouin (WKB) approximation, when the electric field strength is not too large [12].

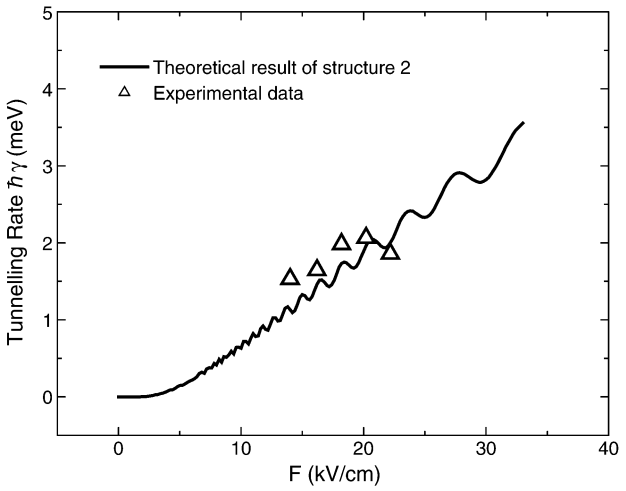

Fig. 3. The tunnelling rate shown by the solid line we calculated using Eq. (4), and the experimental data obtained from Ref. [8] shown by hollow triangles.

It is important to point out that the amplitude of the oscillations predicted by this theory is systematically smaller than the experimental data. This is attributed to a principal limitation of the theory, which assumes tunnelling during different Bloch cycles to be uncorrelated, while there was a weak correlation between tunnelling during subsequent Bloch cycles in experiments [20].

Furthermore, Fig. 3 has been plotted to show the comparison between our calculated results denoted by a solid line and the experimental data denoted by the hollow triangles reported in Ref. [8] for structure 2. It is important to point out that for the case of low electric field the WSL separation eFd is less than the level broadening due to scattering, so the current model based on WSLs is not valid when F is less than about 10 kV/cm. Thus, the broadening mechanism in the low field region is not Zener tunnelling [9]. In the high electric field region (above 15 kV/cm), the agreement between theoretical results and experimental data has been obtained. From these results, we can find that the sudden changing of the THz spectral shapes in high field region is indeed due to the resonant interminiband Zener tunnelling. The discrepancies between theoretical results and experimental data can be attributed to the correlated tunnelling during subsequent Bloch cycles and the transient effects caused by the time-resolved THz spectra.

As we all know, it is meaningful for the observed broadening to Zener tunnelling when a central frequency can be defined. The central frequency versus electric field F is plotted in Fig. 4. In this figure, ω_B is the experimental THz emission central frequency measured from Ref. [8] and $eFd/\hbar$ is the simply expected Bloch frequency. In the low field region (below 10 kV/cm), ω_B is simply set to be $eFd/\hbar$. However, the peak position of the THz spectra in the high field region (above 10 kV/cm) is slightly lower than the value of $eFd/\hbar$, which has been attributed to anticrossing with the WSL states of the second miniband [8].

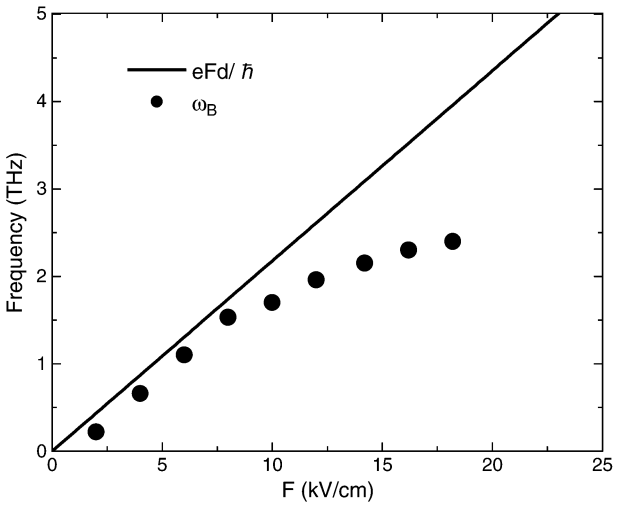

Fig. 4. The comparison between measured THz emission central frequency ω_B (solid circles) with the simply expected Bloch frequency $eFd/\hbar$ (solid line).

4. Summary and conclusion

In summary, we have calculated Zener tunnelling rates between two minibands of various energy band structures by means of quantum-mechanical perturbation theory using Kane functions as base functions. The tunnelling rate increases with the electric field F and shows oscillations as the result of interacting of WSLs between two minibands. The oscillation period increases with electric field and decreases with the miniband-width of the SLs. From our theoretical results, we also find that Zener tunnelling rate increases with the decreasing of the minigap in the low field region. The agreement between the theoretical HWHM and the experimental broadening of THz emission spectrum [8] gives evidence that the sudden changing of THz spectra in the high electric field region is indeed due to the resonant interminiband Zener tunnelling.

Acknowledgments

We gratefully acknowledge financial support from the National Natural Science Foundation of China (No. 60321003). This work was also supported by the SIDA-Swedish Research Links (Grant No. 348-2002-6935).

References

[1] J. Orenstein, A.J. Millis, Science 288 (2000) 468.
[2] T. Nakazato, M. Oyamada, N. Niimura, S. Urasawa, O. Konno, A. Kagaya, R. Kato, T. Kamiyama, Y. Torizuka, Phys. Rev. Lett. 63 (1989) 1245.
[3] U. Happek, A.J. Sivers, E.B. Blum, Phys. Rev. Lett. 67 (1991) 2962.
[4] R.L. Savage, C. Joshi, W.B. Mori, Phys. Rev. Lett. 68 (1992) 946.

[5] C. Waschke, H.G. Roskos, R. Schwedler, K. Leo, H. Kurz, K. Köhler, Phys. Rev. Lett. 70 (1993) 3319.
[6] K. Leo, Bolivar P. Haring, F. Brüggemann, R. Schwedler, K. Köhler, Solid State Commun. 84 (1992) 943.
[7] Y. Shimada, K. Hirakawa, S.-W. Lee, Appl. Phys. Lett. 81 (2002) 1642.
[8] Y. Shimada, K. Hirakawa, M. Odnoblioudov, K.A. Chao, Phys. Rev. Lett. 90 (2003) 046806.
[9] N. Sekine, Y. Shimada, K. Hirakawa, Appl. Phys. Lett. 83 (2003) 4794.
[10] Y. Shimada, N. Sekine, K. Hirakawa, Appl. Phys. Lett. 84 (2004) 4926.
[11] K. Leo, High-Field Transport in Semiconductor Superlattices, Springer-Verlag, Berlin, Heidelberg, 2003.
[12] K.-J. Jin, M. Odnoblyudov, Y. Shimada, K. Hirakawa, K.A. Chao, Phys. Rev. B 68 (2003) 153315.
[13] J. Bleuse, G. Bastard, P. Voisin, Phys. Rev. Lett. 60 (1988) 220.
[14] C. Zener, Proc. R. Soc. London A 145 (1934) 523.
[15] B. Rosam, D. Meinhold, F. Löser, V.G. Lyssenko, S. Glutsch, F. Bechstedt, F. Rossi, K. Köhler, K. Leo, Phys. Rev. Lett. 86 (2001) 1307.
[16] A. Sibille, J.F. Palmier, F. Laruelle, Phys. Rev. Lett. 80 (1998) 4506.
[17] E.J. Halperin, D. Lofgreen, R.K. Kawakami, D.K. Young, L. Coldren, A.G. Gossard, D.D. Awschalom, Phys. Rev. B 65 (2002) 041306.
[18] W.V. Houston, Phys. Rev. 57 (1940) 194.
[19] E.O. Kane, J. Phys. Chem. Solids 12 (1959) 181.
[20] S. Glutsch, Phys. Rev. B 69 (2004) 235317.